CONF-790847--2

HEAVY QUARK-ANTIQUARK BOUND STATES IN THE FRAMEWORK OF QUANTUM CHROMODYNAMICS*

T. D. Viollier+

Center for Theoretical Physics
Laboratory for Nuclear Science and Department of Physics
Massachusetts Institute of Technology
Cambridge, Massachusetts 02139

and

J. Rafelski

CERN, Geneva, Switzerland

Paper submitted to the VIII International Conference on High-Energy Physics and Nuclear Structure, Vancouver, Canada, August 13-17, 1979

+also CERN, Geneva, Switzerland

*This work is supported in part through funds provided by the U.S. Department of Energy (DOE) under contract EY-76-C-02-3069.

CTP# 791
June, 1979

Abstract

Based on the first order running coupling constant $a_\Lambda(q^2)$ we derive in the static limit a quark-antiquark potential. The tachyon pole in $a_\Lambda(q^2)$ leads to a partially confining potential, while the smooth remainder gives rise to a Coulomb like interaction. We impose linear confinement by extrapolating the confining potential linearly for distances $r > r_o$. Thus, aside from the quark masses, m_c and m_b, our model contains two free parameters: (i) the renormalization mass Λ, and (ii) the extrapolation radius r_o. With Λ = 441 MeV, r_o = .378 fm, m_c = 1.525 GeV, and m_b = 4.929 GeV we reproduce the observed orthocharmonium and orthobottomium spectrum very well. This can be viewed as evidence for the validity of the framework of quantum chromodynamics.

1. Introduction

Two families of heavy quark-antiquark bound states, the $J/\psi \equiv (c\bar{c})$ and the $\Upsilon \equiv (b\bar{b})$ resonances, have been discovered. There is a strong theoretical prediction that at least one more family may exist which has a new type of heavy quark t[1] as fundamental building blocks. The spectroscopic properties of these heavy quarkonium states represent a sensitive test for quantum chromodynamics (QCD),[2] the currently accepted gauge theory of strong interactions. In contrast to the light quarks (u, d, s), the nonrelativistic heavy quarks (c, b, t) directly probe the static quark-antiquark potential.

So far, most studies of the J/ψ and Υ systems have been based on a phenomenological approach to the quark-antiquark interaction.[3-7] In particular, the usual Coulomb + linear potential model,[3] though motivated to some extent by QCD, does not include the strong vacuum polarization effects arising from virtual gluons and quarks. This polarizability of the vacuum is reflected e.g. in the concept of asymptotic freedom[8] or in the momentum transfer dependence of the strong coupling "constant"

$$\alpha_\Lambda(q^2) = \frac{1}{B_f \log q^2/\Lambda^2} \quad . \tag{1}$$

Here the constant B_f denotes

$$B_f = (11 - 2/3\, f)/4\pi \tag{2}$$

where the first term represents the gluon contribution and f stands for the number of (massless) quark flavors contributing to the polarizability of the vacuum. From scaling violations in deep inelastic reactions,[9] the renormalization mass Λ is known within the range of 300 MeV $\lesssim \Lambda \lesssim$ 600 MeV.

The running coupling constant $\alpha_\Lambda(q^2)$ can be calculated from the Callan-Symanzik $\beta(\alpha_\Lambda)$-function by integrating the renormalization group equation.[5,10] In this approach Eq. (1) represents only a first order term which includes, however, vacuum polarization effects arising from virtual gluon and quark pairs (Fig. 1). While this approximation is adequate for $\alpha_\Lambda/\pi \ll 1$, it is perhaps no longer justified for large α_Λ's, since then multigluon effects may become relevant. For the present study, we find it reasonable to have our considerations based on the expression (1), primarily in order to assess its range of validity. We will show, however, that Eq. (1), supplemented with the idea of linear confinement,[11] represents already an excellent starting point for the evaluation of the charmonium and bottomium spectra.

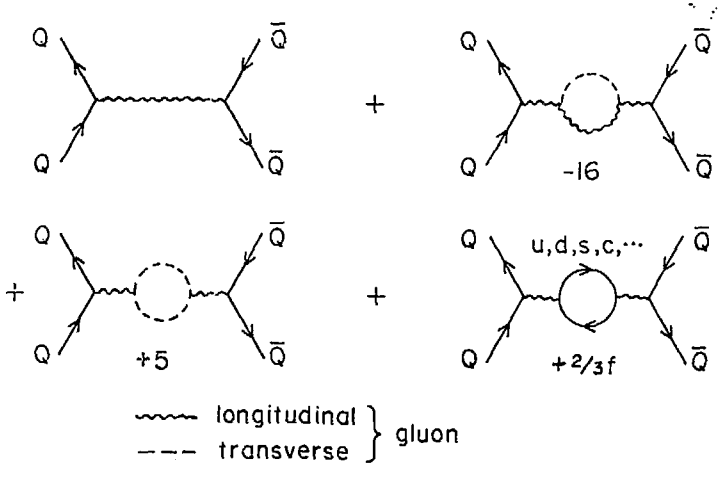

Fig. 1

The Coulomb and first order vacuum polarization contributions to the quark-antiquark interaction. The numbers below the graphs denote their relative contribution.

We describe the nonrelativistic heavy quark-antiquark system in terms of the Schrödinger equation ($\hbar$=c=1)

$$\left(-\frac{1}{m_Q}\nabla^2 + W\right)\psi = E\psi \tag{3}$$

where m_Q is the quark mass, M the mass of the bound state ψ

$$M = 2m_Q + E \tag{4}$$

and (-E) its binding energy. The spin structure of the quark-antiquark interaction $W(\underset{\sim}{r})$ has the general form[12]

$$W(\underset{\sim}{r}) = W_0(r) + W_1(r)\underset{\sim}{L}\cdot\underset{\sim}{S} + W_2(r)S_{12} + W_3(r)\underset{\sim}{\sigma}_1\cdot\underset{\sim}{\sigma}_2 \tag{5}$$

where $\underset{\sim}{L}$ is the orbital angular momentum, S_{12} denotes the tensor operator

$$S_{12} = 3(\underset{\sim}{\sigma}_1\cdot\hat{\underset{\sim}{r}})(\underset{\sim}{\sigma}_2\cdot\hat{\underset{\sim}{r}}) - \underset{\sim}{\sigma}_1\cdot\underset{\sim}{\sigma}_2 \tag{6}$$

and

$$\underset{\sim}{S} = \frac{1}{2}(\underset{\sim}{\sigma}_1 + \underset{\sim}{\sigma}_2) \tag{7}$$

represents the total spin of the quark-antiquark pair.

The details of the spin independent potential $W_o(r)$ are determined by QCD and shall be given further below. If $W_o(r)$ can be represented as a sum of a Lorentz vector and scalar piece

$$W(r) = V(r) + S_o(r) \tag{8}$$

the spin dependent parts are found via nonrelativistic reduction yielding the generalized Breit-Fermi interaction[10]

$$\begin{cases} W_1(r) = \frac{1}{2m_Q^2}\left(\frac{3}{r}\frac{dV_0}{dr} - \frac{1}{r}\frac{dS_0}{dr}\right) \\ W_2(r) = \frac{1}{2m_Q^2}\left(\frac{1}{r}\frac{dV_0}{dr} - \frac{d^2V_0}{dr^2}\right) \\ W_3(r) = \frac{1}{6m_Q^2}\Delta V_0 = \frac{1}{6m_Q^2}\left(\frac{d^2V_0}{dr^2} + \frac{2}{r}\frac{dV_0}{dr}\right) + \text{eventually delta term}. \end{cases} \tag{9}$$

In the present article, we will solve the spin independent problem and treat the spin dependent parts in first order perturbation theory, since terms of the same order in v/c have been already neglected in the central part of the potential.

2. The Quark-Antiquark Potential

The quark-antiquark potential that describes one-gluon-exchange with the vacuum polarization corrections shown in Fig. 1 is given in the static limit by[12]

$$\begin{aligned} U(r) &= -\frac{4}{3}\frac{1}{2\pi^2}\int \frac{\alpha_\Lambda(q^2)}{q^2} e^{-i\underline{q}\underline{r}}\, d^3\underline{q} \\ &= -\frac{4}{3}\frac{2}{\pi}\int_0^\infty \frac{\alpha_\Lambda(q^2)}{q^2}\,\frac{\sin qr}{qr}\, q^2 dq \end{aligned} \tag{10}$$

which is the Fourier transform of the Coulomb propagator dressed with the running coupling constant (1). The singularity in $\alpha_\Lambda(q^2)$ can be easily separated

$$\alpha_\Lambda(q^2) = \alpha_0(q^2) + \alpha_1(q^2) \tag{11}$$

by introducing explicitly the tachyon pole at spacelike momentum transfers $q^2 = \Lambda^2$

$$\alpha_0(q^2) = \frac{\Lambda^2}{B_f\,(q^2-\Lambda^2)}\,. \tag{12}$$

Thus the nonsingular remainder is

$$\alpha_1(q^2) = \frac{1}{B_f}\left(\frac{1}{\log\frac{q^2}{\Lambda^2}} - \frac{\Lambda^2}{q^2-\Lambda^2}\right). \tag{13}$$

The pole term $\alpha_0(q^2)$ will lead to a partially confining potential, whereas the nonsingular remainder $\alpha_1(q^2)$ gives rise to a Coulomb like interaction with variable effective coupling.

Let us first discuss the pole term $\alpha_0(q^2)$. Interpreting the singular integral[10] in terms of a principal value integral

$$U_0(r) = -\frac{4}{3}\frac{2}{\pi} P \int_0^\infty \frac{\Lambda^2}{B_f (q^2-\Lambda^2) q^2} \frac{\sin qr}{qr} q^2 dq, \quad (14)$$

we obtain a positive definite expression

$$U_0(r) = \frac{4}{3}\frac{1}{B_f}\frac{1}{r}(\cos \Lambda r - 1) = \frac{8}{3B_f r}\sin^2\frac{\Lambda r}{2} . \quad (15)$$

For distances $r \ll \Lambda^{-1}$ $U_0(r)$ reduces to

$$U_0(r) \approx \frac{2}{3}\frac{1}{B_f}\Lambda^2 r = a^{-2} r. \quad (16)$$

Using our preferred values, f = 3 and Λ = 441 MeV, the slope of the confining potential turns out to be

$$a^{-2} = \frac{2}{3}\frac{1}{B_f}\Lambda^2 = .18\ GeV^2 \quad (17)$$

consistent with the Coulomb + linear potential.[3] This surprising fact makes it possible to suggest a link between the pole term (15) and confinement. However, our $U_0(r)$ can only

describe partial confinement, since it oscillates reaching its first maximum of roughly 550 MeV at about 1 fm. While the potential (15) is apparently incorrect for large values of r where, according to lattice gauge theories,[11] it should rise linearly, there is reason to believe its structure at short distances. In this spirit, we impose linear confinement by extrapolating $U_0(r)$ linearly for distances $r > r_0$

$$\bar{U}_0(r) = \begin{cases} U_0(r) & r \le r_0 \\ U_0(r_0) + U_0'(r_0)(r-r_0) & r > r_0 \end{cases} . \quad (18)$$

The extrapolation radius r_0 is a phenomenological parameter to be determined from the experimental data.

We now turn to the discussion of the nonsingular remainder

$$U_1(r) = -\frac{4}{3}\frac{1}{B_f}\frac{2}{\pi}\int_0^\infty \left(\frac{1}{\log q^2/\Lambda^2} - \frac{\Lambda^2}{q^2-\Lambda^2}\right)\frac{\sin qr}{qr} dq \quad (19)$$

Using Cauchy's integral theorem, we arrive at

$$U_1(r) = \frac{4}{3}\frac{1}{B_f r} u(\Lambda r) \quad (20)$$

where

$$u(\Lambda r) = \int_0^\infty \frac{e^{-tr} - 1}{\left(\log t^2/\Lambda^2\right)^2 + \pi^2} \frac{dt^2}{t^2} =$$

$$= -\frac{1}{2} + \int_0^\infty \frac{dx}{x^2+\pi^2}\left[e^{-\Lambda r e^{x/2}} + e^{-\Lambda r e^{-x/2}} - 1\right]. \quad (21)$$

This potential is negative definite and gives rise to a Coulomb like interaction which is less singular than the Coulomb potential at short distances.

So far, the quarks contributing to the vacuum polarization have been assumed as massless. While this approximation is adequate for the up and down quarks, it is certainly incorrect for the strange quark. For our purposes, however, it will be sufficient to have a rough estimate of the vacuum polarization effects arising from a massive strange quark. Without detailed justification for this small correction, we therefore replace the constant B_f in eqs. (15) and (20) by a radius dependent B_{eff}

$$\frac{1}{B_{eff}} = \frac{1}{B_2} + \left(\frac{1}{B_3} - \frac{1}{B_2}\right) e^{-2m_s r} . \quad (22)$$

This form guarantees that only up and down quarks contribute for $r \gg (2m_s)^{-1}$

$$\frac{1}{B_{eff}} \approx \frac{1}{B_2} , \quad (23)$$

while at short distances $r \ll (2m_s)^{-1}$ also the strange quark becomes effective

$$\frac{1}{B_{eff}} \approx \frac{1}{B_3} . \quad (24)$$

The exponential range of $B_{eff}^{-1}(r)$ is adjusted to the approximate range of the vacuum polarization potential arising from strange quark-antiquark pairs. The total spin independent potential $W_o(r)$ thus becomes

$$W_o(r) = U_o^{eff}(r) + U_1^{eff}(r) \quad (25)$$

where $U_o^{eff}(r)$ and $U_1^{eff}(r)$ is given by eqs. (15), (18) and (20), replacing B_f by $B_{eff}(r)$.

3. Numerical Results

3.1 The Spectra

We now turn to the discussion of the numerical results. The theoretical description of the states above flavor threshold is unreliable due to the presence of the new channel. We therefore restrict our study to the low-lying states. In order to investigate the contribution of the quarks to the polarizability of the vacuum, we evaluate the charmonium and bottomium spectra for three different potentials, characterized as follows:

(A) two massless and one massive quark
($m_u = m_d = 0$; $m_s = 300$ MeV)

(B) two massless quarks ($m_u = m_d = 0$)

(C) three massless quarks ($m_u = m_d = m_s = 0$)

For charmonium, the three free parameters of the model, Λ, r_o, and m_c, are determined by fitting the 1S, 2S, and 1P levels to the experimental $1^3S_1(3.097)$, $2^3S_1(3.686)$, and to the center of gravity of the $1^3P_{0,1,2}$ levels at 3.523 GeV,[13] respectively, using the potential type A. The fit parameters Λ = 441 MeV, r_o = .378 fm, and m_c = 1.525 GeV, are compatible with what one may expect from other sources.[9] For the bottomium spectrum we use the potential A with the same values of Λ and r_o. The only free parameter left, the bottom quark mass m_b, is adjusted to the experimental 1^3S_1 (9.46) level of bottomium[14] yielding m_b = 4.929 GeV.

In Fig. 2 we have plotted the quark-antiquark potential type A. Here the dotted line denotes the Coulomb like potential $U_1^{eff}(r)$ and the dashed line corresponds to the partially confining potential $U_o^{eff}(r)$. The dashed-dotted line is the linearized confining potential $\bar{U}_o^{eff}(r)$, while the sum $\bar{U}_o^{eff}(r) + U_1^{eff}(r)$ (solid line) represents the potential actually used in the calculations.

In Fig. 3 we show the charmonium spectrum. The excellent agreement between theory and experiment is largely due to the fact that the three lowest levels have been fitted. Thus the only independent tests of the model are the 3^3S_1 (4.040) level which is unreliable, since it is far above charm threshold, and the $1^3D_1(3.772)$ level which cannot be compared directly to the calculated center of gravity of the $1^3D_{1,2,3}$ levels.

The real test of quantum chromodynamics comes with the bottomium spectrum shown in Fig. 4. Our calculations agree very well with the observed bottomium spectrum and thus confirm the reliability of the first order QCD potential. Here the experimental 2^3S_1 (10.02) and 3^3S_1 (10.38) levels are below bottom threshold and represent therefore a conclusive test of our model. In fact, this potential that includes both concepts, asymptotic freedom and linear confinement, does a much better job than e.g. the Coulomb + linear potential. We recall here that the original Coulomb + linear potential[3] fails by about 150 MeV in the description of the 2S and 3S bottomium states.

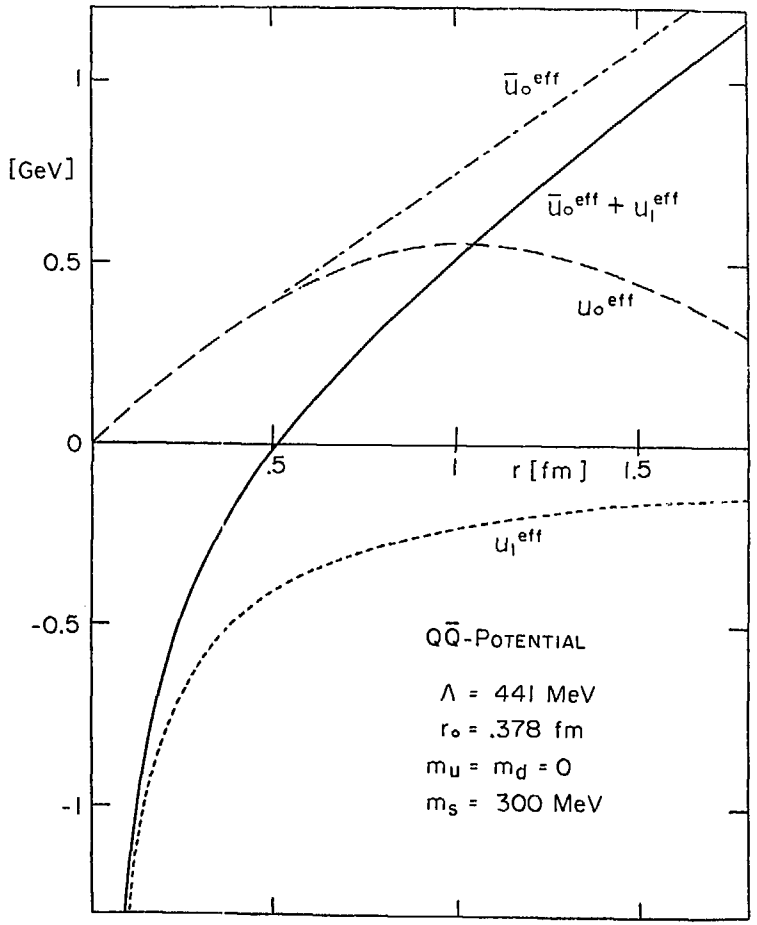

Fig. 2

The Quark-Antiquark Potential type A

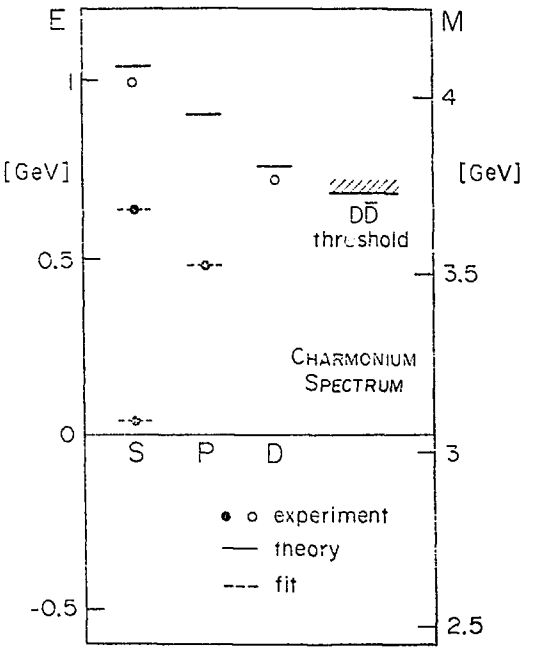

Fig. 3

The charmonium spectrum calculated with the potential type A

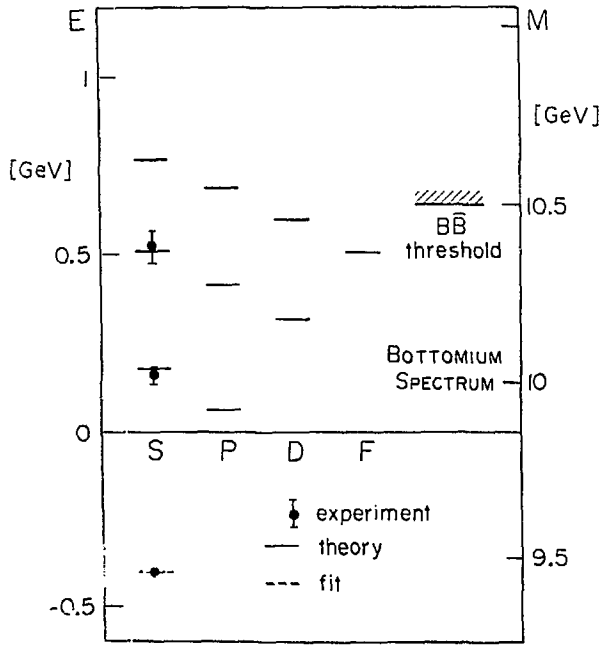

Fig. 4

The bottomium spectrum calculated with the potential type A

The spectra calculated with the potentials type A, B, and C are compared in table 1 and 2. The massive strange quark influences only the low-lying levels, as can be deduced by comparing the spectra type A (massive strange quark) and B (no strange quark). This is not a surprise, since the potentials, A and B, differ only in the short-range strange quark contribution. However, if one replaces the massive quark (type A) by a third massless quark (type C), all levels are shifted by an appreciable amount. Thus for the charmonium and bottomium states, the major quark contribution to the polarizability of the vacuum comes from the (massless) up and down quarks and the (massive) strange quark affects only the low-lying levels up to about 10 MeV for charmonium and 40 MeV for bottomium.

state	M[GeV]			
	experiment	A	B	C
3S	(4.040±.010)	4.090	4.093	4.132
2S	3.686±0.003	3.686*	3.690	3.706
1S	3.097±0.002	3.097*	3.110	3.088
2P		3.951	3.951	3.983
1P	3.523±.005	3.523*	3.524	3.531
1D	(3.772±.006)	3.806	3.804	3.829

Table 1

The charmonium spectrum calculated with the potential A, B, and C (* ≡ fit).

state	M[GeV]			
	experiment	A	B	C
4S		10.628	10.632	10.655
3S	10.38±0.04	10.370	10.376	10.384
2S	10.02±0.02	10.039	10.050	10.037
1S	9.46±0.01	9.460*	9.498	9.441
3P		10.543	10.546	10.565
2P		10.275	10.279	10.282
1P		9.921	9.931	9.911
2D		10.456	10.457	10.472
1D		10.176	10.179	10.176
1F		10.366	10.366	10.376

Table 2

The bottomium spectrum calculated with the potential A, B, and C (* ≡ fit).

3,2 Spindependent Terms

We now turn to the discussion of the current data on the spindependent interaction. The spinorbit and tensor splittings of the P-levels in charmonium are well established. Using Eq.(5) we obtain in first order perturbation theory

$$\begin{cases} M(1^3P_2) = M(1^3P) + W_1(1P) - \frac{2}{5} W_2(1P) \\ M(1^3P_1) = M(1^3P) - W_1(1P) + 2 W_2(1P) \\ M(1^3P_0) = M(1^3P) - 2 W_1(1P) - 4 W_2(1P) . \end{cases} \quad (26)$$

From the experimental P-levels $1^3P_2(3.554)$, $1^3P_1(3.508)$, and $1^3P_0(3.413)$[13] one can deduce the center of gravity of the triplet P states (Table 1)

$$M(1^3P) = 3.523 \text{ GeV} \quad (27)$$

and the expectation values of the spin-orbit and tensor interaction (Table 3)

$$\begin{cases} W_1(1P) = 35 \text{ MeV} \\ W_2(1P) = 10 \text{ MeV} . \end{cases} \quad (28)$$

Similarly, we have for the D-states in first order

$$\begin{cases} M(1^3D_3) = M(1^3D) + 2 W_1(1D) - \frac{4}{7} W_2(1D) \\ M(1^3D_2) = M(1^3D) - W_1(1D) + 2 W_2(1D) \\ M(1^3D_1) = M(1^3D) - 3 W_1(1D) - 2 W_2(1D) . \end{cases} \quad (29)$$

From the observed $1^3D_1(3.772)$ level and the theoretical estimate $M(1^3D) = 3.806$ GeV one concludes

$$3 W_1(1D) + 2 W_2(1D) = 34 \text{ MeV}(??) . \quad (30)$$

However, this relation is unreliable, since it depends critically on the unchecked value of $M(1^3D)$.

The hyperfine splittings of the 1S, 2S and 1D states are given in first order by

$$\begin{cases} M(1^3S_1) - M(1^1S_0) = 4 W_3(1S) \\ M(2^3S_1) - M(2^1S_0) = 4 W_3(2S) \\ M(1^3D) - M(1^1D_2) = 4 W_3(1D) . \end{cases} \quad (31)$$

Here the experimental situation is less clear. If we interpret the states at 2.830(?), 3.454(?) and 3.590 GeV(??) as the para-charmonium states 1^1S_0, 2^1S_0, and 1^1D_2, respectively, we obtain for the expectation values of the spin-spin potential

$$\begin{cases} W_3(1S) = 66.8 \text{ MeV}(?) \\ W_3(2S) = 58 \text{ MeV}(?) \\ W_3(1D) = 54 \text{ MeV}(??) . \end{cases} \quad (32)$$

Here we have used the observed orthocharmonium states 1^3S_1 (3.097), $2^3S_1(3.686)$ and theoretical $1^3D(3.806)$ state. None of the supposed paracharmonium states is really well-established, and therefore, the experimental values for the matrix elements

(32) should not be taken too seriously. However, if the interpretation of the 2.830 and 3.454 states is correct, the quark model is in trouble because of the necessary large M1-transition rates from the J/ψ and ψ' to these states. Moreover, if the new state at 3.590 GeV is really a 1^1D_2 state, there is apparently a state independent contribution to the matrix elements (32) which is hard to explain within the framework of Eq.(9).

Our calculated matrix elements are shown in Table 3 for charmonium and Table 4 for bottomium based on the potentials A, B, and C. Here the spin independent potential W_o is assumed to be of vector type

$$\begin{cases} V_o = \bar{U}_o^{eff} + U_1^{eff} \\ S_o = 0 \end{cases} \quad . \tag{33}$$

While the theoretical tensor splitting $W_2(1P)$ is more or less consistent with the experiment, we are left with a serious discrepancy in the spinorbit splitting $W_1(1P)$. Of course, $W_1(1P)$ could be fitted to the experimental value by introducing a scalar component in the confining potential

$$\begin{cases} V_o = \bar{U}_o^{eff}\eta + U_1^{eff} \\ S_o = (1-\eta)\bar{U}_o^{eff} \end{cases} \tag{34}$$

at the expense of a still smaller tensor splitting $W_2(1P)$. Going even a step further, one can allow for an anomalous chromomagnetic moment in order to fit both, $W_1(1P)$ and $W_2(1P)$[15].

state	experiment			A			B			C		
	W_1	W_2	W_3	W_1	W_2	W_3	W_1	W_2	W_3	W_1	W_2	W_3
3S	0	0		0	0	15.4	0	0	14.5	0	0	16.4
2S	0	0	58.0?	0	0	20.0	0	0	18.9	0	0	21.5
1S	0	0	66.8?	0	0	36.6	0	0	33.8	0	0	38.9
2P				59.3	6.5	6.8	56.7	6.1	6.8	64.5	7.0	7.6
1P	35	10		76.1	8.2	8.9	72.9	7.7	8.9	83.1	8.9	10.0
1D	$W_1+\frac{2}{3}W_2$ = 11.3??		5422	37.1	3.4	5.6	36.6	3.3	5.7	41.2	3.7	6.3

Table 3

The experimental and theoretical expectation values of the spin dependent potentials for charmonium (in MeV).

state	A			B			C		
	W_1	W_2	W_3	W_1	W_2	W_3	W_1	W_2	W_3
4S	0	0	3.0	0	0	2.8	0	0	3.2
3S	0	0	3.8	0	0	3.5	0	0	4.0
2S	0	0	5.4	0	0	4.9	0	0	5.7
1S	0	0	13.4	0	0	11.6	0	0	13.6
3P	13.9	1.7	1.2	12.8	1.6	1.1	14.8	1.8	1.3
2P	16.9	2.1	1.4	15.6	1.9	1.4	18.0	2.2	1.6
1P	24.4	3.1	2.0	22.0	2.7	1.9	25.7	3.2	2.2
2D	7.3	.8	.8	6.9	.7	.8	8.0	.9	.9
1D	8.9	1.0	1.0	8.5	.9	1.0	9.7	1.1	1.1
1F	5.2	.5	.7	5.1	.5	.7	5.8	.6	.8

Table 4

The theoretical expectation values of the spin dependent potentials for bottomium [in MeV].

At this stage, however, where the spinorbit splitting is the only established discrepancy between theory and experiment, the introduction of two arbitrary parameters is hardly justified, since it would drastically reduce the predicting power of the theory. An alternative explanation of the discrepancy is that the potentials $V_o(r)$ and $W_o(r)$ differ appreciably in the domain .3 fm $\lesssim r \lesssim$ .5 fm. Clearly spin effects are quite sensitive to the detailed structure of the vector part of the potential $V_o(r)$ in this region.

From the matrix elements given in Table 4 and Eqs. (26) and (29) we can deduce the energy levels of the 1P and 1D states in orthobottomium

$$M(1^3P_{0,1,2}) = (9.860, 9.903, 9.944)\ \text{GeV} \tag{35}$$

$$M(1^3D_{1,2,3}) = (10.147, 10.169, 10.193)\ \text{GeV}. \tag{36}$$

However, as we have noticed earlier in this section, we should not trust this prediction too much, except for the fact that the splittings are much smaller than for charmonium.

3.3 Leptonic Decays

An interesting check of the model are the leptonic decay widths usually calculated through the van Royen-Weisskopf[16] formula

$$\Gamma(n^3S_1 \to \ell^+\ell^-) = \frac{16\pi\alpha^2}{M(n^3S_1)^2} |\psi_n(0)|^2 e_Q^2 . \tag{37}$$

Here α denotes the fine structure constant, e_Q is the charge of the quark in units of e, and $\psi_n(0)$ is the n^3S_1- state wave function at the origin. It has been shown that this equation is subject to large radiative corrections which tend to suppress the leptonic widths drastically. In fact, Eq.(37) should read

$$\Gamma(n^3S_1 \to \ell^+\ell^-) = \frac{16\pi\alpha^2}{M(n^3S_1)^2} |\psi_n(0)|^2 e_Q^2 F(m_Q). \tag{38}$$

The correction factor $F(m_Q)$ can be evaluated to first order in α_Λ[17] giving

$$F(m_Q) = 1 - \frac{4}{3}\frac{4}{\pi}\alpha_\Lambda(-m_Q^2) \tag{39}$$

where $\alpha_\Lambda(-m_Q^2)$ denotes the strong coupling constant at time-like momentum transfers $q^2 = -m_Q^2$. Since the correction is rather large, we may conclude that the first order result is unreliable. Thus, at the present stage, $F(m_Q)$ is best kept as a free parameter to be determined from the charmonium and bottomium data.

In tables 5 and 6 the leptonic decay widths are shown for

charmonium and bottomium, respectively. Note the theoretical widths of the ground states have been fitted to their experimental values by introducing the scale factors

$$F(m_c) = .55 \quad \text{and} \quad F(m_b) = .67 \tag{40}$$

In first order these correspond to the coupling constants at

$$\alpha_\Lambda(-m_c^2) = .27 \quad \text{and} \quad \alpha_\Lambda(-m_b^2) = .22 , \tag{41}$$

respectively, which are somewhat larger than expected but not completely unreasonable. Thus only the widths of the excited states are meaningful in our comparison of the theoretical and experimental data in Tables 5 and 6. The widths of the 2S states agree very nicely with the experimental data.

state	$\Gamma(n^3S_1 \to e^+e^-)$ [keV] experiment	A	B	C
3S	.75±.15	1.3	1.3	1.4
2S	2.1±.3	2.0	1.9	2.1
1S	4.8±.6	4.8*	4.4	4.9

Table 5

The leptonic widths of the charmonium states calculated using eq. (38) with $F(m_c^2)$ = .55 (*) and 1.0

state	$\Gamma(n^3S_1 \to \ell^+\ell^-)$ [keV]			
	experiment	A	B	C
4S		.3	.2	.3
3S		.3	.3	.3
2S	.4±.2	.5	.5	.5
1S	1.3±.2	1.3*	1.1	1.3

Table 6

The leptonic widths of the bottomium states calculated using eq. (38) with $F(m_b) = .67$ (* ≡ fit)

5.4 [illegible]

For completeness, we also include the electric dipole transition rates. In nonrelativistic QCD the rates for the electric dipole transitions are given by [illegible]

$$\begin{cases} \Gamma(E1, 2^3S_1 \to 1^3P_J) = \frac{4}{27}(2J+1)e_Q^2\alpha\left[M(2^3S_1) - M(1^3P_J)\right]^3 R^2_{1P,1S} \\ \Gamma(E1, 1^3P_J \to 1^3S_1) = \frac{4}{9}e_Q^2\alpha\left[M(1^3P_J) - M(1^3S_1)\right]^3 R^2_{1S,1P} \end{cases} \quad (43)$$

where $R_{n'\ell',n\ell}$ is the electric dipole radial element

$$R_{n'\ell',n\ell} = \int_0^\infty u_{n'\ell'}(r)\, r\, u_{n\ell}(r) r^2 dr, \quad (44)$$

and $u_{n\ell}(r)$ the radial wave function. Using the experimental masses of the 1^3S_1, 2^3S_1, and $1^3P_{J=0,1,2}$ states, respectively, the 2S-1P transition rates

$$\Gamma(E1, 2^3S_1 \to 1^3P_{0,1,2}) = (40, 58.70)\ \text{keV} \quad (45)$$

are a factor 2 - 3 larger than the corresponding transition rates of (17-8) keV. We can interpret this discrepancy as an indication that the "real" size of charmonium may be smaller than our model predicts. Alternatively, relativistic effects could easily reduce the rates by a factor of 2. For the 1^3P_J transition rates we find

$$\Gamma(E1, 1^3P_{0,1,2} \to 1^3S_1) = (194, 428, 588)\ \text{keV}. \quad (46)$$

We now turn to the magnetic dipole transitions. The theoretical description of the forbidden transitions is uncertain due to coherent relativistic effects. We therefore restrict ourselves to the allowed magnetic transitions

$$\Gamma(M1, n^3S_1 \to n^1S_0) = \frac{4}{3}\frac{e_Q^2}{m_Q^2}\alpha\left[M(n^3S_1) - M(n^1S_0)\right]^3 \tag{46}$$

Assuming that the 1^1S_0 and 2^1S_0 states are at 2.951 and 3.606 GeV, respectively, as predicted by our model, we obtain

$$\Gamma(M1, 1^3S_1 \to 1^1S_0) = 5.8 \text{ keV} \tag{47}$$

which is still larger than the accepted experimental upper limit of 1.1 keV for this transition. The theoretical 2S-transition rate of

$$\Gamma(M1, 2^3S_1 \to 2^1S_0) = 1 \text{ keV} \tag{48}$$

is not in contradiction with the experiment.

4. Final Remarks

We have presented a description of heavy quark-antiquark bound states in the framework of quantum chromodynamics. Our results reproduce the observed orthocharmonium and orthobottomium spectra very well. The excellent agreement not only confirms the reliability of the perturbative approach to QCD and asymptotic freedom, but also establishes a strict quantitative relation between the parameters of the theory and experiment. We obtain a renormalization mass of λ=441 MeV, consistent with estimates from deep inelastic reactions.[43] The quark masses, m_c=1.525 and m_b=4.920 GeV, as well as the phenomenological extrapolation radius r_0=.378 fm seem reasonable. The strength parameter

$$B_f = \left(11 - \tfrac{2}{3}f\right)/4\pi \tag{49}$$

is most sensitive to the gluon contribution to the polarizability of the vacuum. Thus our results confirm that the exchanged gluons are indeed the gauge bosons of a $SU(N_{color})$ gauge theory with N_{color}=3. As far as the quark contribution is concerned, our calculations are consistent with three quark flavors: two massless up and down quarks and a massive strange quark of m_s=300 MeV. However, it is also possible to reproduce the charmonium and bottomium data neglecting the strange quark vacuum polarization. In fact, using λ=472 MeV, r_0=.402 fm, m_c=1.505 GeV, and m_b=4.909 GeV, we obtain a similar fit to the experimental spectra with f=2, as well.

The electric dipole transition rates and the leptonic widths are in reasonable agreement with the experimental data. However, the detailed spin structure of the quark-antiquark interaction as well as the M1 transition rate to the para-charmonium ground state still remain to be understood.

Concluding we would like to emphasize that, if the top quark exists, the toponium spectrum will be a crucial test for the model. Assuming a top quark mass of $m_t \gtrsim 15$ GeV, toponium will probe much more the domain that can be described by perturbative QCD and that is presumably less sensitive to phenomenological modifications at large distances.

References

1. See e.g.: Y. Hara, Rapporteur talk XIX Int. Conf. on High Energy Physics, Tokyo, August 1978.
2. See e.g.: W. Bardeen, H. Fritzsch, and M. Gell-Mann, in Scale and Conformal Symmetry and Hadron Physics (ed. R. Gatto, New York, 1973).
3. E. Eichten et al, Phys. Rev. Letters 34 (1975)369; E. Eichten and K. Gottfried, Phys. Letters 66B (1977) 286.
4. C. Quigg and J.L. Rosner, Phys. Letters 71B (1977) 153; 72B (1978) 462.
5. W. Celmaster, H. Georgi and M. Machacek, Phys. Rev. D17 (1978) 879; 17 (1978) 886; W. Celmaster and F. Henyey, Phys. Rev. D18 (1978) 1688.
6. G. Bhanot and S. Rudaz, Phys. Letters 78B (1978) 119.
7. J.L. Richardson, SLAC preprint SLAC-PUB-2229.
8. H.D. Politzer, Phys. Rev. Letters 30 (1973) 1346. D.J. Gross and F. Wilczek, Phys. Rev. D8 (1973) 3633; Phys. Rev. Letters 30 (1973) 1434.
9. See e.g.: O. Nachtmann, Proc. of the Int. Symp. on Photon and Lepton Physics, Hamburg, August 1977. A. De Rújula, H. Georgi, and H.D. Politzer, Ann. Phys. (N.Y.) 103 (1977) 315. J.G.H. de Groot et al, Phys. Letters 82B (1979) 292,456.

10. M. Gell-Mann and F. Low, Phys. Rev. 95 (1954) 1300.
K. Symanzik, Comm. Math. Phys. 18 (1970) 227.
C. Callan, Phys. Rev. D2 (1970) 1541.

11. J. Kogut and L. Susskind, Phys. Rev. D9 (1974) 3501;
D11 (1975) 395; K. Wilson, Phys. Rev. D10 (1974) 2445.

12. See e.g.: J.D. Jackson, Proc. 1976 Summer Instutue on
Particle Physics, SLAC Report No. 198 (1976) p.147.

13. N. Barash-Schmidt et al, Phys. Letters 75B (1978).
R. Brandelik et al, Phys. Letters 76B (1978) 361.
P.A. Rapidis et al, Phys. Rev. Letters 39 (1977) 526;
39 (1977) 974E.

14. Ch. Berger et al, Phys. Letters 76B (1978) 243.
C.W. Darden et al, Phys. Letters 76B (1978) 246.
S.W. Herb et al, Phys. Rev. Letters 39 (1977) 252.
W.R. Innis et al, Phys. Rev. Letters 39 (1977)1240.
J.K. Bienlein et al, DESY Report (1978).

15. H.J. Schnitzer, Phys. Letters 65B (1976) 239.

16. R. van Royen and V.F. Weisskopf, Nuovo Cimento, 50A (1967)
617.

17. R. Barbieri et al, Nucl. Phys. B105 (1976) 125.